The EMBO Journal Vol. 22 No. 14 pp. 3635–3644, 2003

slalom encodes an adenosine 3′-phosphate 5′-phosphosulfate transporter essential for development in *Drosophila*

Florian Lüders, Hiroaki Segawa[1], David Stein[2], Erica M.Selva[3,4], Norbert Perrimon[3], Salvatore J.Turco[1] and Udo Häcker[5]

Department of Cell and Molecular Biology, BMC B13, Lund University, 22184 Lund, Sweden, [1]Department of Biochemistry, University of Kentucky Medical Center, 800 Rose Street, Lexington, KY 40536, [2]Section of Cell and Developmental Biology and Institute for Cellular and Molecular Biology, University of Texas at Austin, 1 University Station C0930, Austin, TX 78712-0253 and [3]Department of Genetics, Harvard Medical School, HHMI, 200 Longwood Avenue, Boston, MA 02118, USA

[4]Present address: Department of Biological Sciences, University of Delaware, 325 Wolf Hall, Newark, DE 19716, USA

[5]Corresponding author
e-mail: udo.haecker@medkem.lu.se

Sulfation of all macromolecules entering the secretory pathway in higher organisms occurs in the Golgi and requires the high-energy sulfate donor adenosine 3′-phosphate 5′-phosphosulfate. Here we report the first molecular identification of a gene that encodes a transmembrane protein required to transport adenosine 3′-phosphate 5′-phosphosulfate from the cytosol into the Golgi lumen. Mutations in this gene, which we call *slalom*, display defects in Wg and Hh signaling, which are likely due to the lack of sulfation of glycosaminoglycans by the sulfotransferase *sulfateless*. Analysis of mosaic mutant ovaries shows that *sll* function is also essential for dorsal–ventral axis determination, suggesting that *sll* transports the sulfate donor required for sulfotransferase activity of the dorsal–ventral determinant *pipe*.

Keywords: glycosaminoglycan/Hedgehog/Pipe/sulfation/Wingless

Introduction

Secreted signaling molecules of the FGF, Hh, TGF-β and WNT families rely on proteoglycans (PGs) for efficient activation of their respective signaling pathways (reviewed in Perrimon and Bernfield, 2000). PGs consist of secreted or transmembrane core proteins to which glycosaminoglycan (GAG) side chains are attached at specific consensus sites. In *Drosophila*, the secreted PG perlecan (Park *et al*., 2003), the transmembrane PG syndecan (Spring *et al*., 1994) and two members of the glypican family of glycosylphosphatidylinositol (GPI) anchored PGs have been identified. Phenotypes associated with loss of function mutations of the glypican-encoding genes *dally* (Nakato *et al*., 1995) and *dally-like* (*dlp*) (Khare and Baumgartner, 2000; Baeg *et al*., 2001) have revealed the requirement of these PGs for efficient activation of several signal transduction pathways.

The function of PGs is critically dependent on the integrity of the attached GAGs. GAGs are unbranched polysaccharide chains, which are synthesized on proteoglycan core proteins in the Golgi and undergo complex modification reactions before the PG to which they are attached is transported to the cell surface. In the case of glypican, heparan sulfate (HS) chains, which consist of a sugar backbone of alternating units of *N*-acetylglucosamine (GlcNAc) and glucuronic acid (GlcA), are synthesized on the core protein. The nucleotide sugar substrates for this reaction are synthesized in the cytoplasm and must be transported into the Golgi. In *Drosophila*, the activated precursor UDP-GlcA is synthesized from UDP-glucose by the enzymatic activity of the *sugarless* (*sgl*) gene product (Binari *et al*., 1997; Häcker *et al*., 1997; Haerry *et al*., 1997), a homolog of mammalian UDP-glucose dehydrogenases. The gene product of *fringe connection* (*frc*), a predicted ER/Golgi multipass transmembrane protein, has been shown to transport UDP-GlcA and UDP-GlcNAc from the cytosol into the Golgi (Goto *et al*., 2001; Selva *et al*., 2001). Mutations in either gene severely affect the Wg and FGF signaling pathways. Elongation of the HS chains requires the activity of HS polymerases. *tout-velu* (*ttv*) encodes a protein with homology to the mammalian HS copolymerase *EXT1* and has been demonstrated to be required specifically for Hh signaling (Bellaiche *et al*., 1998). Subsequent to their synthesis, GAGs undergo multiple modifications such as epimerization and sulfation. Mutations in *sulfateless* (*sfl*), a homolog of vertebrate *N*-deacetylase/*N*-sulfotransferases, lead to a severe reduction in the activity of the Wg, Hh and FGF signaling pathways (Lin and Perrimon, 1999; Lin *et al*., 1999). A characteristic feature of all mutations in genes involved in GAG biosynthesis is that their segment polarity phenotypes can be rescued by ectopic expression of *wg* or *hh*, suggesting that GAGs are not essential components of the respective signaling cascades but accessory factors most likely required for the proper distribution of extracellular signaling molecules throughout morphogenetically active tissues *in vivo*.

GAGs have also been proposed to play a role in the determination of the dorsal–ventral (D/V) axis of the *Drosophila* embryo (Sen *et al*., 1998). The D/V polarity of the embryo is established during oogenesis by asymmetric expression of the key D/V determinant *pipe* (*pip*) in the follicle cell epithelium. *pip* expression in the ventral follicle cell layer is necessary and sufficient to trigger a serine–protease cascade in the perivitelline space, which leads to the generation of an active ligand for the transmembrane receptor Toll (Tl). Activation of Tl on

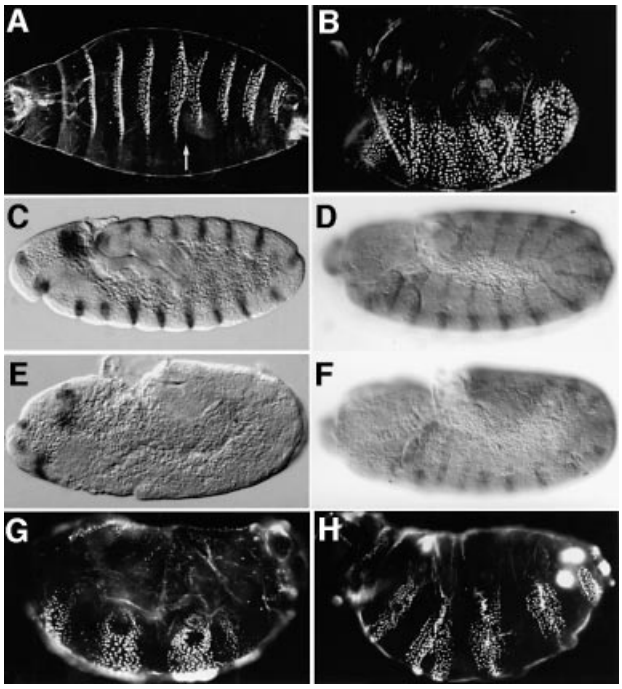

Fig. 1. Embryonic phenotypes of *sll* mutants. (**A**) Cuticle phenotype of a sll^{7E18} homozygous embryo derived from heterozygous parents. Note occasional fusion of denticle belts (arrow). (**B**) Cuticle phenotype of a sll^{7E18} homozygous embryo derived from a female carrying sll^{7E18} germ-line clones (referred to as *sll* null mutant hereafter). Note the complete absence of smooth cuticle on the ventral side. (**C**) Wg expression in a wild-type embryo at stage 10. (**D**) En expression in a wild-type embryo at stage 11. (**E**) Wg expression in thoracic and abdominal segments of a sll^{7E18} null mutant is completely abolished at stage 10. (**F**) En expression in thoracic and abdominal segments of a sll^{7E18} null mutant is dramatically decreased at stage 11. (**G**) Expression of a *UAS-wg* transgene using a *prd-Gal4* driver line in sll^{7E18} null mutants. Note the development of smooth cuticle in alternating segments. (**H**) Expression of a *UAS-hh* transgene using a *prd-Gal4* driver line in sll^{7E18} null mutants. Note the development of smooth cuticle in alternating segments. Anterior is to the left and dorsal side up in all panels, except (A), which is a ventral view.

the ventral side of the embryo results in a gradient of nuclear localization of the transcription factor Dorsal, which patterns the D/V axis (reviewed in Amiri and Stein, 2002). Based on sequence similarity to a family of vertebrate enzymes and its localization in the Golgi apparatus, *pip* has been hypothesized to encode a heparan sulfate 2-*O*-sulfotransferase. However, neither the enzymatic activity nor the substrate specificity of *pip* have been demonstrated directly.

Sulfation of secreted molecules occurs in the Golgi and requires the high-energy sulfate donor adenosine 3′-phosphate 5′-phosphosulfate (PAPS) to be present within that organelle. In *Drosophila*, PAPS is synthesized in the cytoplasm by PAPS-synthetase (Jullien *et al*., 1997), which incorporates both ATP-sulfurylase and adenosine 5′-phosphosulfate-kinase (APS-kinase) activity. PAPS must be transported into the Golgi thereafter (Lyle *et al*., 1994) to serve as a substrate for sulfotransferases. Here, we report the first molecular identification and functional characterization of a PAPS transporter. Mutations in this gene, which we call *slalom* (*sll*), are associated with defects in multiple signaling pathways, including Wg and Hh signaling. A phenotypic analysis suggests that the effects of *sll* on signal transduction are caused by its requirement for GAG modification. We present evidence that *sll* is also required to supply PAPS to the machinery initiating the establishment of embryonic D/V polarity, supporting the view that Pipe protein is a sulfotransferase.

Results

Identification of slalom

The *sll* mutant was identified in a genetic screen for zygotic lethal mutations associated with maternal effect phenotypes. Homozygous sll^{7E18} larvae, derived from heterozygous parents, do not hatch and produce cuticles with occasional fusions of denticle belts (Figure 1A). Homozygous sll^{7E18} larvae derived from mothers carrying sll^{7E18} germ-line clones (referred to as *sll* null mutants throughout the text) exhibit a fully penetrant segment polarity phenotype (Figure 1B) similar to that seen in *wg* or *hh* mutants, suggesting that *sll* may have a function in the Wg and/or Hh signaling pathways.

In wild-type embryos, pair-rule genes initiate the expression of *wg* and its target gene, the homeodomain transcription factor *engrailed* (*en*), at the cellular blastoderm stage. After germ-band extension, the expression of *wg* and *en* is maintained by a positive feedback loop between the Wg and Hh signaling pathways. In mutants of segment polarity genes essential for Wg signal transduction, the expression of *wg* and *en* fades at stage 10. To confirm that *sll* is involved in segment polarity determination we stained sll^{7E18} null mutants for Wg (Figure 1E) or En (Figure 1F) protein. The expression of both genes is initiated normally in sll^{7E18} null mutants (not shown) but fades prematurely compared with wild type. However, in contrast to null mutations in other segment polarity genes, such as *dishevelled* (*dsh*) or *armadillo* (*arm*) (Peifer *et al*., 1991), *en* expression is maintained significantly longer in sll^{7E18} mutants, until stage 12. This phenotype is also seen in mutations that disrupt enzymes required for the biosynthesis of heparan sulfate proteoglycans (HSPGs), such as *sugarless* (*sgl*), *sulfateless* (*sfl*) or *fringe connection* (*frc*) (Binari *et al*., 1997; Häcker *et al*., 1997; Haerry *et al*., 1997; Selva *et al*., 2001).

In contrast to the segment polarity defects caused by mutations in core components of the Wg signaling pathway, such as *dsh*, the phenotype of *sgl*, *sfl* or *frc* mutants can be rescued by overexpression of either *wg* or *hh*. To test whether this is the case for *sll*, we expressed *UAS-wg* or *UAS-hh* transgenes in *sll* null mutants using a *prd-Gal4* driver. Larval cuticles from embryos expressing *wg* (Figure 1G) or *hh* (Figure 1H) in a pair-rule pattern show rescue of the segment polarity phenotype in alternating segments, corresponding to the domains of *prd* expression. These observations show that the Wg and Hh signaling pathways can be activated in the absence of *sll* function, and suggest that *sll* may play a role in the biosynthesis of GAGs.

sll is required for Wg and Hh signaling

The Wg and Hh signaling pathways are engaged in a positive feedback loop during patterning of the ventral embryonic epidermis (reviewed in Perrimon, 1994), which makes it difficult to distinguish which of the pathways requires *sll* activity. Therefore, the question of whether *sll*

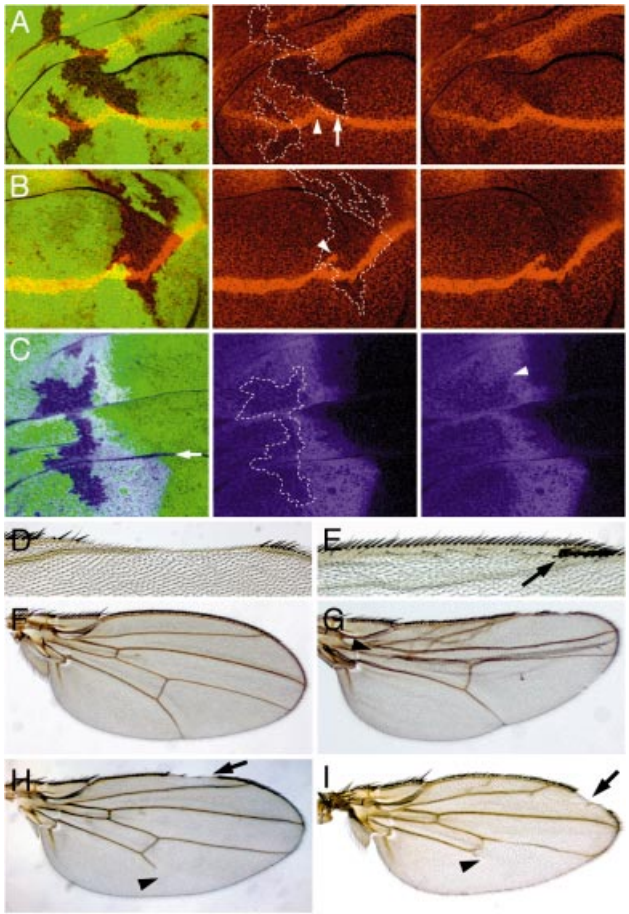

Fig. 2. Role of *sll* during wing development. (**A** and **B**) Examples of Wg distribution (red) in wing imaginal discs carrying sll^{7E18} mutant clones. (A, center and right panel) Same as left panel showing only Wg expression. Compare Wg levels adjacent to the D/V boundary inside (arrow) and outside the clone. Note the reduction of Wg protein levels in sll^{7E18} mutant cells. The D/V boundary often shows a change in direction associated with sll^{7E18} mutant clones (arrowhead in center panel). (B, center and right panel) Same as left panel showing only Wg expression. Note bifurcation of the D/V boundary inside the sll^{7E18} mutant clone (arrowhead in center panel). Homozygous sll^{7E18} mutant cells are marked by the absence of GFP (green) expression in left panels and by the dashed outlines in center panels of (A), (B) and (C). (**C**) Ci distribution (purple) in wing imaginal discs carrying sll^{7E18} mutant clones. The center and right panels are the same as the left panel showing only Ci expression. Note that Ci expression is moderately reduced in sll^{7E18} mutant cells receiving the Hh signal. The arrowhead in the right panel indicates the region where strongest reduction is seen. (D–G) Wing phenotypes associated with sll^{7E18} mutant clones. (**D**) Wing exhibiting a gap in the anterior margin. (**E**) Bifurcation of the anterior wing margin (arrow). (**F**) Wild-type wing. (**G**) Wing showing reduction in region between wing veins L3 and L4 (arrowhead). (**H**) Wing of $dally^{527}/dally^{sem}$ transheterozygote. Note truncation of wing vein L5 (arrowhead). (**I**) Wing of $sll^{l(3)142214}/sll^{7E18}$ transheterozygote showing gaps in the margin (arrow) and truncation of wing vein L5 (arrowhead) very similar to (H).

function is required for Wg or Hh signaling was addressed during wing imaginal disc development, where the two pathways act in clearly distinguishable patterning processes. In the wing imaginal disc, *wg* is expressed in a stripe of cells along the D/V boundary of the wing. A Wg protein gradient emanating from *wg*-expressing cells is required to pattern the wing margin (reviewed in Irvine, 1999). When clones of sll^{7E18} mutant cells crossing the D/V boundary were stained for Wg protein (Figure 2A and B), no change in Wg protein levels was observed in *wg*-expressing cells. However, despite their close proximity to the Wg source, sll^{7E18} mutant cells immediately adjacent to the D/V boundary showed a significant reduction in Wg protein levels, leading to a disruption of the gradient (Figure 2A). The wings of adults carrying sll^{7E18} mutant clones frequently exhibited gaps in the anterior margin (Figure 2D). Similar gaps were also observed in $sll^{L(3)142214}/sll^{7E18}$ transheterozygous adults, which are viable but show patterning defects due to reduced *sll* activity (arrow in Figure 2I). These observations suggest a role for *sll* in Wg distribution and are consistent with an involvement of *sll* in GAG metabolism.

Furthermore, *wg* expression in wing imaginal discs frequently exhibited changes of direction or bifurcations of the D/V boundary (Figure 2A and B, arrowheads in center panels) in association with sll^{7E18} mutant clones, suggesting a role for *sll* during establishment of compartment boundaries at an early stage of imaginal disc development. In adult wings, these abnormalities in *wg* expression resulted in the production of extra margin bristles inside the wing blade (Figure 2E, arrow).

We also stained wing discs carrying sll^{7E18} mutant clones for the protein product of the Hh target gene *Cubitus interruptus* (*Ci*) (Motzny and Holmgren, 1995) (Figure 2C). sll^{7E18} mutant clones located in the anterior compartments of wing discs showed a moderate reduction in Ci protein levels, indicating reduced Hh signaling activity. Consistent with this observation, adult wings carrying sll^{7E18} mutant clones frequently showed a reduction in the region between longitudinal veins L3 and L4, which has been demonstrated to be sensitive to Hh signaling (Figure 2G, arrowhead) (Mullor *et al*., 1997; Strigini and Cohen, 1997). In addition, wings carrying sll^{7E18} mutant clones, or $sll^{L(3)142214}/sll^{7E18}$ wings, form ectopic vein tissue associated with wing vein L2 (Figure 2G). This phenotype cannot be explained by defects in Wg or Hh signaling and suggests that *sll* is also required for the activity of other signal transductions pathways, such as the TGF-β pathway. These results suggest that, similar to genes encoding proteoglycan core proteins, such as *dally*, or genes involved in GAG biosynthesis, such as *sgl*, *frc* or *sfl*, *sll* function is required for the activity of several signaling pathways.

Molecular identification of sll

The original ethyl methane sulfonate-induced allele sll^{7E18} was used to identify a non-complementing P-element insertion allele $sll^{l(3)24533}$. Embryos maternally and zygotically mutant for $sll^{l(3)24533}$ showed a cuticle phenotype similar to, though weaker than, sll^{7E18} (Figure 3A). The P-element in $sll^{l(3)24533}$ is inserted in the 5′-UTR of a putative protein-encoding transcription unit. In another, independently identified P-element-induced allele, $sll^{l(3)142214}$, the transposon was also found inserted in the 5′-UTR of the same transcription unit (Figure 3C). Furthermore, we determined the nucleotide sequence of this transcription unit in the sll^{7E18} allele and detected a nonsense mutation which leads to termination of the open reading frame (ORF) after 42 amino acids. The truncated ORF contains none of the predicted transmembrane regions of the encoded protein, suggesting that sll^{7E18} is a null allele (Figure 3C).

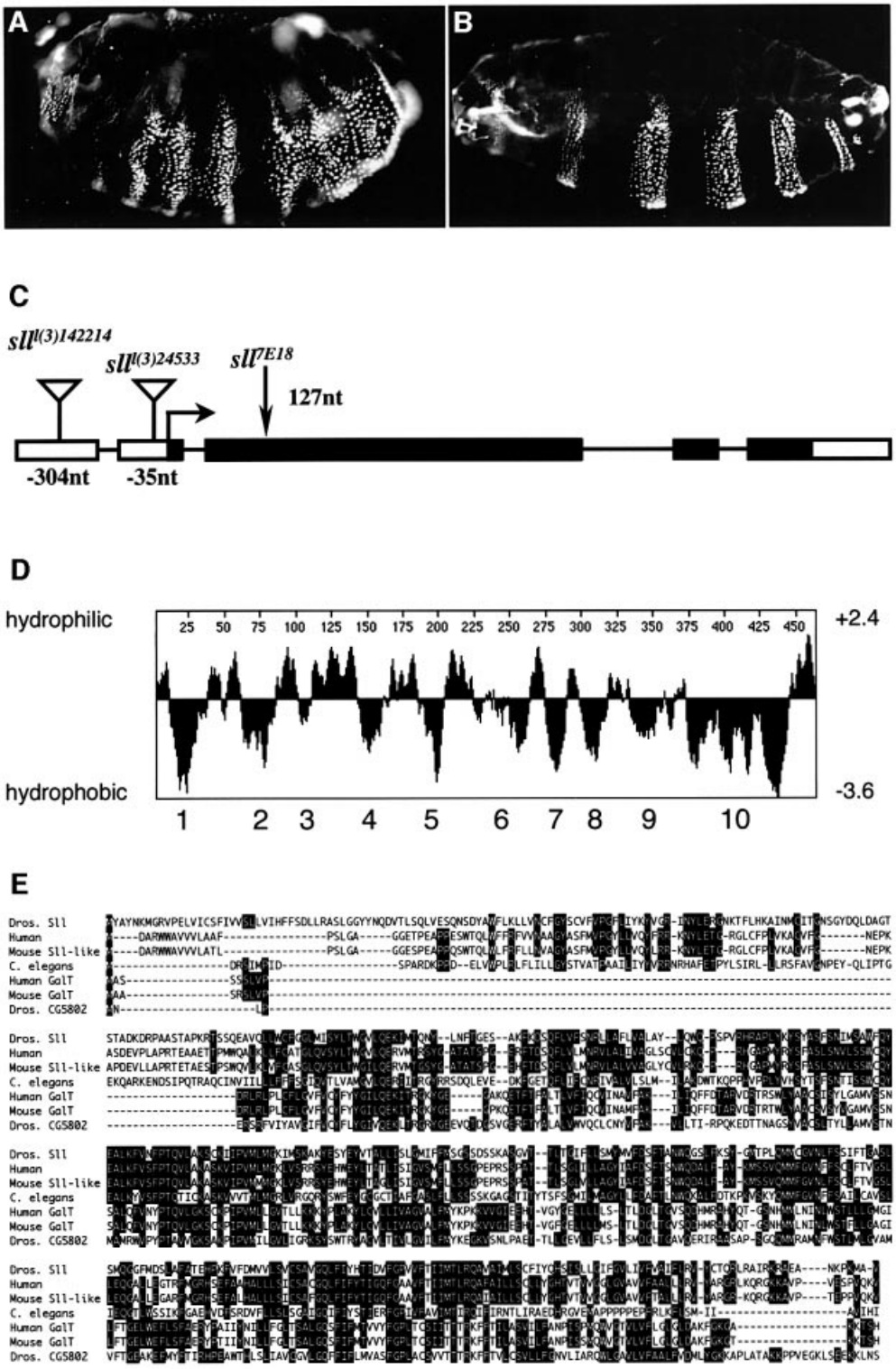

Fig. 3. Molecular identification of *sll*. (**A**) Cuticle phenotype of $sll^{l(3)24533}$ maternal and zygotic mutant larva. Note the occasional development of smooth cuticle in some segments, indicating that $sll^{l(3)24533}$ is not a null allele. (**B**) Pair-rule segmentation phenotype of sll^{7E18} null mutant larvae expressing a *UAS-sll* transgene under the control of a *prd*-Gal*4* driver line. (**C**) Gene structure of *sll*. The P-element insertions in the *sll* transcript are located 304 nucleotides [$sll^{l(3)142214}$] and 35 nucleotides [$sll^{l(3)24533}$], respectively, upstream of the start codon. The sll^{7E18} allele has a C to T transition creating a nonsense mutation in the 42nd codon (nucleotide 127) of the reading frame. (**D**) The *sll* cDNA encodes a putative hydrophobic protein of 465 amino acids (52 kDa) with at least 10 predicted transmembrane spanning regions. (**E**) Homology alignment of Sll with a putative human protein (39.4%) (Protein Data Bank accession No. AK075456), a putative mouse Sll-like protein (41.1%) (BC036992), *Caenorhabditis elegans* gene M03F8.2 (28.8%) (NM072147), a putative human galactose transporter UGTREL1 (28.6%) (NM005827), a putative mouse galactose transporter (29.2%) (NM016752) and the *Drosophila* gene CG5802 (21.3%). Amino acid identity to Sll is indicated by percentage values in brackets. Protein accession numbers are in brackets.

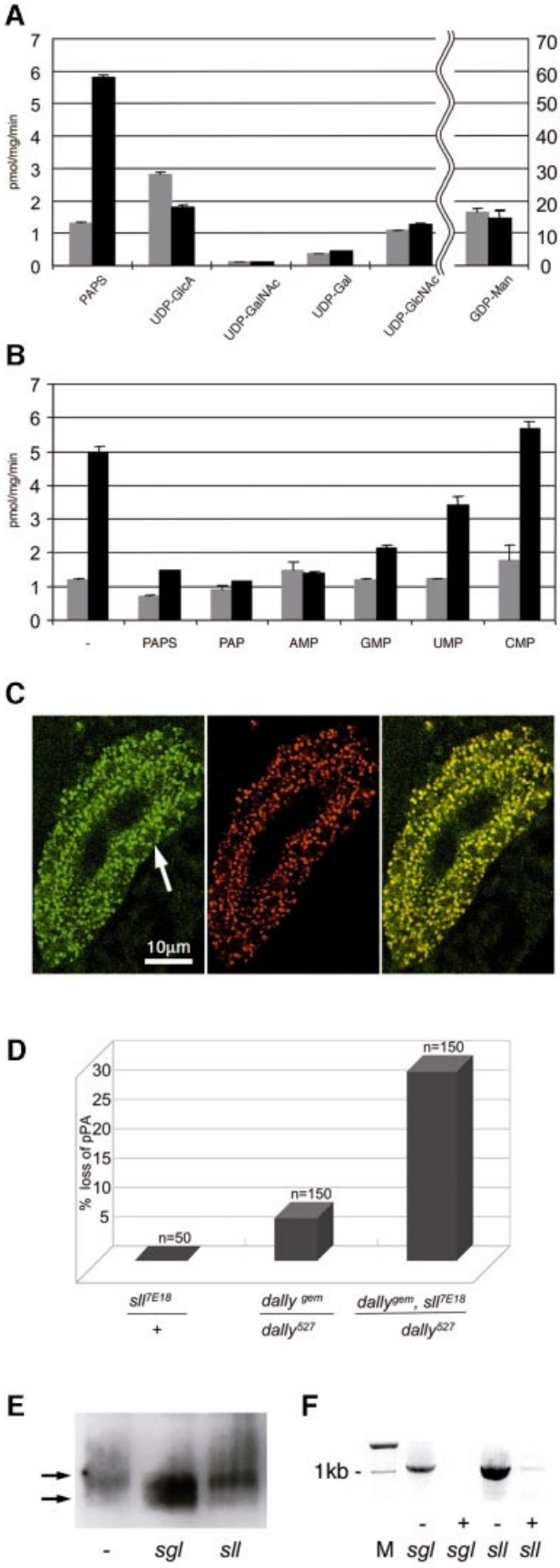

To demonstrate that this transcription unit represents the *sll* gene, a putative *UAS-sll* transgene was introduced into the genome and expressed in *sll* mutants. Expression of *UAS-sll* in sll^{7E18} null mutants using a *prd-Gal4* driver resulted in larval cuticles with a pair-rule-like segmentation pattern (Figure 3B), indicating that the *UAS-sll* transgene was responsible for the rescuing activity. Embryos homozygous for sll^{7E18}, carrying an *actin-Gal4* driver and a *UAS-sll* transgene, developed into viable and fertile adults with no phenotypic abnormalities, showing that *UAS-sll* identifies the *sll* gene. This result further suggests that *sll* can be ubiquitously expressed throughout development with no deleterious effects for the organism, and that *sll* function is largely dosage independent.

sll encodes a PAPS transporter located in the Golgi apparatus

A hydrophobicity analysis of the putative Sll protein predicted a hydrophobic polypeptide with at least 10 transmembrane regions, which is a structural characteristic of many nucleotide–sugar transporters (Figure 3D) (reviewed in Gerardy-Schahn *et al*., 2001). A BLAST search of non-redundant protein databases, available at NCBI, with the Sll sequence revealed that Sll is conserved throughout the animal kingdom (Figure 3D), as well as in plants, and shares nearly 40% of amino acid sequence identity with predicted mouse and human proteins of unknown function. Sll is also similar to mammalian proteins that have been classified as nucleotide–sugar transporters on the basis of their homology (Ishida *et al*., 1996) to the human UDP-galactose transporter hUGT (Miura *et al*., 1996). However, Sll itself has no significant sequence similarity to hUGT. While these data suggest that Sll encodes a transmembrane transporter, they leave open what substrate Sll may be transporting.

In order to demonstrate directly that Sll has transporter activity, and to determine its substrate specificity, an

Fig. 4. *sll* encodes a PAPS transporter. (**A**) Transport activity of Sll for various nucleotide–sugar substrates and PAPS. The microsomes from *sll*-transfected *S.cerevisiae* were prepared and assayed for transport of the designated nucleotides at a concentration of 5 mM, as described in Materials and methods. Transport activity is shown in picomoles of substrate transported per milligram of microsomes per minute. Transport of GDP-Man is shown on a 10-fold higher scale compared with all other substrates. (**B**) Effect of nucleotide addition on PAPS transport into microsomal vesicles. Microsomal vesicles were prepared from *sll*-transfected *S.cerevisiae* and assayed for PAPS ^{35}S-transport activity in the presence of various nucleotide monophosphates at 100 µM concentration. In (A) and (B), the gray bars indicate transport by microsomes isolated from *S.cerevisiae* and transfected with empty vector. Black bars indicate transport by microsomes isolated from *S.cerevisiae* and transfected with a *sll*-expression vector. (**C**) The left panel shows the expression of Sll in salivary glands. Note the perinuclear localization of the staining. The arrow points to the nucleus of one cell visible as a dark area. The bar is 10 µm long. The center panel shows the expression of a *Drosophila* Golgi specific protein in salivary glands. The right panel was obtained by merging the left and center panels. Note the extensive co-localization of staining. (**D**) Genetic interaction between *dally* and *sll* in loss of the posterior postalar bristle (pPA). (**E**) Western blot analysis of HA–Dally from S2 cells incubated with buffer (–) or dsRNA specific for *sugarless* (*sgl*), or *slalom* (*sll*). Upper arrows indicate the size of HA–Dally in untreated cells. The lower arrow indicates the size of HA–Dally after RNAi treatment against *sgl* (center lane) or *sll* (right lane). (**F**) Amplification of *sgl* or *sll* RNA by RT–PCR from S2 cells incubated with buffer (–) or dsRNA (+) specific for *sugarless* (*sgl*) or *slalom* (*sll*). M, DNA size marker.

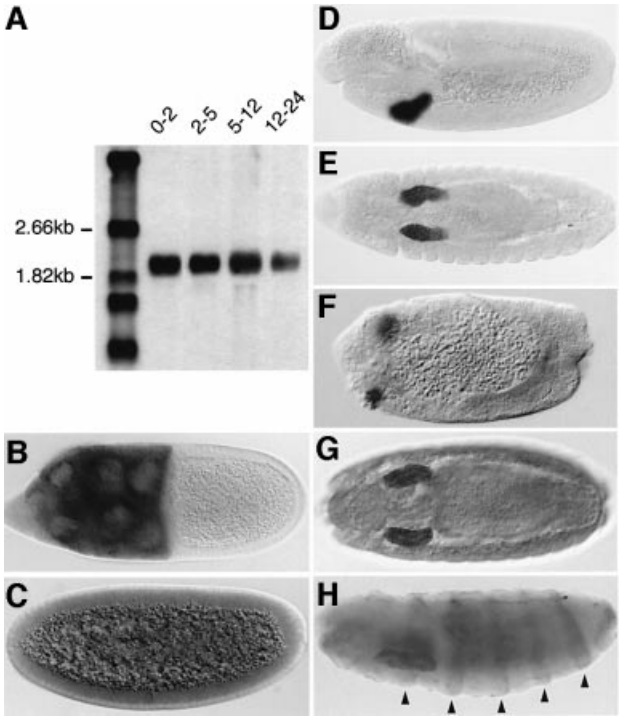

Fig. 5. Expression of *sll* mRNA during embryonic development. (**A**) Northern blot showing expression of *sll* transcripts at different time intervals during embryogenesis. (**B**) Maternal expression of *sll* RNA in the nurse cells of the germline during oogenesis. (C–F) *In situ* hybridization of *sll* RNA to wild-type (C–E) and sll^{7E18} mutant (F) embryos. (**C**) Maternal expression of *sll* RNA in the syncytial blastoderm embryo (stage 4). (**D**) Zygotic expression of *sll* RNA is first detected in the salivary gland placodes at stage 11. (**E**) Salivary gland specific expression of *sll* RNA at stage 14. (**F**) Expression of *sll* RNA in the salivary gland placodes of a sll^{7E18} null mutant at stage 11. (**G**) Expression of Sll protein in the salivary glands of a wild-type embryo. (**H**) Expression of Sll protein in a *prd-Gal4/UAS-sll* embryo showing that the α-Sll antibody recognizes Sll specifically. Arrowheads indicate expression in epidermal stripes in the abdominal region. (C, D, F and H) Lateral view. (E and G) Ventral view. Anterior is to the left.

in vitro vesicle transport assay was used to examine the ability of Sll to facilitate the transport of defined nucleotide substrates into *Saccharomyces cerevisae* microsomes. Heterologous expression of *sll* in yeast was favored over other systems since we have successfully used procedures for transfection of nucleotide–sugar genes, high-level preparation of sealed microsomal vesicles and nucleotide–sugar assays in this organism (Segawa *et al*., 2002). In vesicles derived from cells transfected with a *sll*-expression construct, a 5-fold increase in the uptake of PAPS was detected. Import of several other nucleotide–sugars did not increase after *sll* expression (Figure 4A). We attribute the background in the control cells to glycosylation reactions, such as mannosylation of dolichol using GDP-Man on the outer surface of the microsomal vesicles (Hirschberg and Snider, 1987). Importantly, the *sll*-dependent PAPS transport activity could be efficiently competed by structurally similar substrate analogs but not by more distantly related nucleotide monophosphates, confirming that the transport was specific (Figure 4B).

PAPS is synthesized in the cytoplasm and serves as a substrate for sulfotransferases during the post-translational modification of macromolecules in the Golgi. Therefore, the result that *sll* encodes a PAPS transporter suggested that Sll should be localized to the Golgi membranes. To address this question, we raised peptide antibodies against Sll. Localization of Sll in salivary glands of wild-type embryos, using Sll antiserum, showed a punctate staining pattern in the perinuclear region of cells (Figure 4C, left panel). Co-staining of salivary glands with antibodies against an endogenous Golgi protein (Stanley *et al*., 1997) (Figure 4C, center panel) revealed extensive co-localization of the two proteins (Figure 4C, right panel), indicating that Sll is a resident Golgi protein. Together, these data suggest that Sll encodes a nucleotide transporter required to translocate the high-energy sulfate donor PAPS into the lumen of the Golgi.

Requirement of sll for proteoglycan function

Several lines of evidence suggest that *sll* interferes with Wg and Hh signaling due to its requirement for GAG modification. In order to confirm these findings we examined genetic interactions between *sll* and the heparan sulfate proteoglycan *dally*, which has previously been implicated in Wg signaling (Lin and Perrimon, 1999; Tsuda *et al*., 1999). Among other functions, *Dally* is required for the development of a subset of sensory bristles on the notum which form in, or immediately adjacent to, *wg*-expressing cells (Fujise *et al*., 2001). Of these macrochaetae, pPA is the one most sensitive to *wg* activity. In adults, transheterozygous for the hypomorphic *dally* alleles $dally^{527}$ and $dally^{gem}$, pPA is absent from 5% of all individuals. When one copy of sll^{7E18} is introduced into these flies, the fraction of individuals that lack pPA climbs to 30% (Figure 4D), showing that *dally* and *sll* act synergistically in the loss of the pPA macrochaeta. $dally^{527}/dally^{gem}$ adults also display defects in wing patterning. In addition to notches in the margin (Figure 2H, arrow), the wings of these mutants show a truncation of the longitudinal vein L5 (Figure 2H, arrowhead). Very similar defects are also seen in wings of $sll^{l(3)142214}/sll^{7E18}$ transheterozygotes (Figure 2I). Together, these data suggest that *sll* function is required for the post-translational modification of heparan sulfate proteoglycans such as *dally*, which are in turn essential for the activity of several extracellular ligand-dependent signaling pathways including the Wg and Hh pathways.

The influence of *sll* on post-translational modification of Dally was examined in a *Drosophila* Schneider (S2) cell assay. S2 cells were transfected with a hemagglutinin-tagged *dally* (*HA-dally*) transgene and the expression of several genes involved in GAG metabolism was subjected to RNA interference (RNAi) mediated inhibition (reviewed in Hannon, 2002). Changes in the mobility of HA–Dally due to altered GAG modification were visualized by SDS–PAGE and western blotting. The synthesis of GAG chains on Dally creates a higher molecular weight population of Dally molecules, which are visible as a smear above the main Dally band (Figure 4E, left lane). Following incubation of cells with double-stranded RNA (dsRNA) specific for *sgl*, the amount of higher molecular weight molecules of Dally is significantly reduced and a lower molecular weight band of *HA-dally* appears (Figure 4E, center lane). These data suggest that a significant fraction of Dally molecules is not properly GAG modified when *sgl* activity is compromised. When

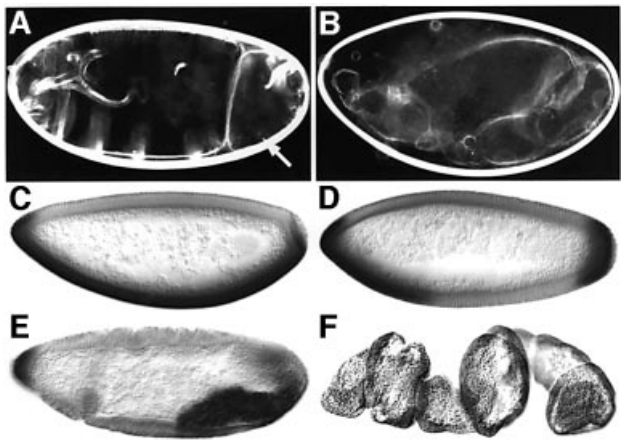

Fig. 6. Role of *sll* in the follicle cell epithelium. (**A** and **B**) Examples of cuticle phenotypes of embryos derived from females carrying sll^{7E18} mutant clones in the follicle cell epithelium. Note the absence of ventral denticle belts in posterior abdominal segments (arrow in A) and the complete dorsalization of the cuticle in (B). (**C**) Twi expression in wild type at the cellular blastoderm stage (stage 5). (D–F) Examples of alterations in expression of the ventral marker Twi in embryos derived from females carrying sll^{7E18} mutant clones in the follicle epithelium. (**D**) Dorsalization in the abdominal region. (**E**) Dorsalization in the gnathal and thoracic region. (**F**) Complete dorsalization of the entire embryo. Anterior is to the left, dorsal side up.

S2 cells were incubated with dsRNA specific for *sll* (Figure 4E, right lane), no change in the mobility of HA–Dally was seen, although *sll* mRNA levels were strongly reduced, as confirmed by RT–PCR (Figure 4F). These observations are consistent with the view that *sll* (Figure 4E, lane) does not interfere with the synthesis of GAG chains on the Dally core protein but is required only for their subsequent sulfation.

sll expression in the germline and in the embryo

The expression profile of *sll* transcripts was first analyzed by northern blotting, which showed that *sll* is expressed throughout embryogenesis (Figure 5A). During oogenesis, *sll* is expressed strongly in the nurse cells of the germline, confirming that *sll* transcripts are maternally contributed to the egg (Figure 5B). *In situ* hybridization to whole-mount embryos detected a low level of ubiquitously expressed maternal *sll* mRNA at the syncytial blastoderm stage (Figure 5C). Zygotic *sll* expression was first detectable after germ-band elongation in the invaginating salivary gland placodes (Figure 5D and E). *sll* remains expressed predominantly in this tissue throughout embryogenesis, but low-level expression below the detection threshold may be present throughout the embryo. *sll* mRNA is also detectable in salivary gland placodes in sll^{7E18} null mutant embryos (Figure 5F), consistent with the molecular defect found in this mutant. Immunohistochemical stainings of wild-type embryos with Sll antibodies confirmed that Sll protein distribution coincides with the expression of *sll* transcripts (Figure 5G). In *prd-Gal4/UAS-sll* embryos, Sll is also detected in epidermal stripes corresponding to the *prd* expression domains, demonstrating that the antibody specifically recognizes Sll (Figure 5H).

sll is required for D/V axis determination

Two other *Drosophila* genes, *windbeutel* (*wbl*) (Nilson and Schüpbach, 1998) and *pip* (Sen *et al*., 1998), are predominantly expressed in the salivary glands during embryogenesis. While the function of these genes in the salivary glands is unclear, both are also required for the establishment of the D/V axis of the egg. During oogenesis, *pip* is expressed specifically in the ventral follicle cell epithelium, where it is involved in the generation of a localized signal triggering the D/V signaling cascade. It encodes a protein with similarity to vertebrate heparan sulfate 2-*O*-sulfotransferases. However, the enzymatic activity of Pip has not been demonstrated directly.

The similarities in the expression patterns of *pip* and *sll*, as well as the molecular functions of both genes, raised the possibility that *sll* function might also be required for D/V axis determination. To test this hypothesis, females carrying *sll* mutant follicle cell clones were generated and phenotypes associated with these clones were analyzed. Cuticles developed from eggs laid by these females frequently exhibited dorsalization of varying severity, ranging from partial and spatially restricted (Figure 6A, arrow) to complete loss of ventral structural elements (Figure 6B). Consistent with the cuticle phenotypes, the ventral mesodermal marker *twist* (Figure 6C) often showed discontinuities, or total loss of expression, in embryos produced by females carrying mosaic ovaries (Figure 6D–F). These data strongly suggest that *sll* activity is required for activation of the D/V signaling cascade initiated by *pip*. To investigate whether the requirement of *sll* in D/V polarity is mediated by GAGs, we generated follicle cell clones homozygous mutant for sgl^{08310} or frc^{00073}. Despite the fact that the ability of sgl^{08310} or frc^{00073} mutant cells to synthesize GAGs is severely reduced, D/V polarity defects similar to those in *sll* mutant clones could not be detected (data not shown). This suggests that GAGs, such as heparan sulfate, chondroitin sulfate or dermatan sulfate, which require GlcA for their formation, may not play a role in D/V axis determination but that *sll* function may be required for sulfation of a different substrate of *pip* in this process.

Discussion

Molecular identification of PAPS translocators

The sulfation of macromolecules is carried out by sulfotransferases in the Golgi and constitutes an important step in the post-translational modification of proteins and the maturation of GAGs in higher organisms. All sulfotransferase reactions require the high-energy donor PAPS. PAPS is synthesized via the sequential actions of ATP sulfurylase and APS kinase in the cytoplasm, and subsequently must be translocated into the Golgi for utilization by luminal sulfotransferases (Capasso and Hirschberg, 1984; Lyle *et al*., 1994). We report the first molecular identification of a PAPS transporter in eukaryotes and demonstrate the importance of sulfate transport into the lumen of the Golgi for pattern-formation processes during development.

The *sll* sequence is unique in the *Drosophila* genome, but homologs are found throughout the animal kingdom, including mice and humans. Proteins with PAPS transport activity have previously been purified from mammalian cells, but their molecular identity has remained elusive. The size of these mammalian PAPS translocators has been reported as 75 or 230 kDa, respectively (Mandon *et al*.,

1994; Ozeran *et al*., 1996), neither of which corresponds to the predicted 47 kDa of mammalian Sll homologs. One possible explanation for this could be that these proteins may be post-translationally modified in a manner that accounts for the size discrepancy. The high degree of conservation between *sll* and its mammalian homologs suggests that they are true orthologs; however, the final evaluation of this will have to await functional characterization of the mammalian proteins.

sll and growth factor signaling

The phenotypical analysis of *sll* mutants shows that *sll* function is required for Wg and Hh signaling, and suggests that *sll* may also play a role in the activation of other signaling pathways, such as the TGF-β pathway and possibly others. The broad requirement for *sll* raises the question of how sulfation influences the function of multiple secreted signaling factors. Proteins entering the secretory pathway are ubiquitously sulfated on specific tyrosine residues. However, according to sulfation consensus prediction algorithms, neither Wg nor Hh is predicted to be a substrate for tyrosine sulfation (see 'Sulfinator' at http://www.expasy.org/tools/sulfinator/) (Monigatti *et al*., 2002). In addition, our overexpression experiments show that *wg* and *hh* have the ability to at least partially activate their respective signaling cascades in *sll* mutants, which would be unlikely if the signaling factors themselves were non-functional due to lack of sulfate modification. Therefore, it is unlikely that lack of tyrosine sulfation of either Wg or Hh proteins is responsible for the defects in Wg or Hh signaling pathways in *sll* mutants.

The Wg and Hh signaling pathways are activated through interaction of secreted ligands with their respective cell surface receptors. This activation relies on the action of GAGs attached to proteoglycan core proteins of the glypican family (Lin and Perrimon, 1999). In the case of Wg, the proteoglycans are thought to act as coreceptors, retaining the ligand at the cell surface in the vicinity of its receptor. Hh has been proposed to depend on GAGs for efficient transport to its target cells. In the absence of functional GAGs, the signaling molecules are not present in sufficiently high concentrations at the receptor to activate the signal transduction pathway. This defect can be compensated by overexpression of the signaling molecule. Therefore, a characteristic feature of mutations in genes involved in GAG metabolism is that their segment polarity defects can be rescued by overexpression of the ligand. Our data show that Wg protein levels and Hh signaling activity are reduced in *sll* mutant clones. The segment polarity defects of *sll* mutants can be rescued by overexpression of *wg* or *hh*. In addition *sll* and *dally* mutants affect Wg signaling synergistically. Our data also suggest that the ability of cells to sulfate GAGs is dramatically reduced in *sll* mutants because the sulfate donor necessary for *sfl* to modify the polysaccharide chains cannot be transported into the Golgi in sufficient amounts. Taken together, these observations strongly suggest that lack of functional GAGs is responsible for the segment polarity defects in *sll* mutants.

Interestingly, the overall size of sugar chains attached to the glypican Dally does not appear to be affected in *sll* mutants. Consistent with this result, it has been observed that the overall level of HS, which is reduced to trace amounts in the *sgl* mutant that affects GAG biosynthesis, is not markedly changed in *sfl* mutants, which should affect sulfate modification but not synthesis of GAG chains (Toyoda *et al*., 2000). However, it cannot be excluded that residual sulfation of GAGs occurs in the cell culture assay owing to incomplete inhibition of the PAPS transport activity of *sll* by dsRNA interference. However, the phenotypic analysis of *sll* suggests that *sll* function is essential for at least two sulfotransferases, *sfl* and *pip*, and that the GAG chains present in *sll* mutants are not able to fulfill their normal function owing to altered sulfation patterns.

sll and D/V patterning

The signal determining the D/V axis of the *Drosophila* embryo is produced by a proteinase cascade active in the perivitelline space of the egg chamber during oogenesis. Activation of this cascade requires localized expression of *pip* in the ventral follicle cells of the ovarian egg chamber in which the egg is constructed, but the mechanism leading to activation remains enigmatic. *pip* has significant similarity to a family of mammalian heparan sulfate 2-*O*-sulfotransferases; however, the enzymatic activity of *pip* has not been demonstrated directly. Our data show that transport of the sulfate donor PAPS into the Golgi is essential for establishment of the D/V axis. The requirement of PAPS for D/V patterning strongly supports the notion that sulfotransferase activity is an essential feature of *pip* function.

This view is also supported by the specific expression patterns of *pip* and *sll* during development. In the embryo, both genes are highly expressed in the developing salivary glands. Another gene involved in PAPS biosynthesis, PAPS synthetase, is also highly expressed in salivary glands (Jullien *et al*., 1997), suggesting that these genes act together in a common pathway providing the sulfate donor for the modification of macromolecules produced in the salivary glands in late embryos and larvae.

Interestingly, the defects in D/V polarity associated with *sll* mutants are not observed in mutants of the UDP-glucose dehydrogenase *sgl* or the UDP-glucuronic acid transporter *frc*. The activity of both genes is required for the formation of GAGs, such as heparan sulfate, chondroitin sulfate or dermatan sulfate, and levels of these GAGs are dramatically reduced in *sgl* mutants (Toyoda *et al*., 2000). These observations support the possibility that GAGs may not play a role in D/V axis determination and that, despite its homology to heparan sulfate 2-*O*-sulfotransferases, *pip* may be required for sulfation of a non-GAG substrate. This view is also consistent with the highly restricted expression pattern of *pip*, which suggests that *pip* is not generally involved in GAG modification.

The central position of *sll* in sulfate metabolism along the secretory pathway makes it an interesting tool for the identification of developmental pathways sensitive to sulfate modification. Our results demonstrate that several cell–cell communication pathways are critically dependent on the sulfation of macromolecules, and highlight the importance of sulfation during pattern formation and development.

Materials and methods

Molecular biology

Genomic DNA flanking *sll* P-element insertions was recovered by plasmid rescue (Huang *et al*., 2000). Insertion sites were determined by nucleotide sequencing of plasmid rescue DNA fragments. Insertion points were determined to be nucleotide 140633 in AE003718.2 for $sll^{l(3)24533}$ and nucleotide 140365 in the same genomic segment for $sll^{l(3)142214}$. The *sll* cDNA SD04670 (DDBJ/EMBL/GenBank accession No. AI533003), which is 1.9 kb long and contains an ORF for a protein of 465 amino acids, was obtained from the *Drosophila* gene collection (BDGP). The point mutation in sll^{7E18} is a C to T transition at nucleotide 127 of the ORF and was identified by PCR amplification of the *sll* locus from sll^{7E18} mutants and subsequent nucleotide sequencing. The *UAS-sll* transgene was produced by cloning the *Eco*RI–*Spe*I fragment of SD04670 into pUASP (Rorth, 1998).

Genetics

The sll^{7E18} mutation is located at 90B3-4 on the third chromosome. The P-element insertion allele $sll^{l(3)24533}$ was identified by complementation analysis. To demonstrate that the lethality of $sll^{l(3)24533}$ is associated with the P-element insertion, the transposase source Δ2–3 was used to mobilize the transposon. This led to excision of the P-element and reversion of the lethality, demonstrating that $sll^{l(3)24533}$ is responsible for the mutation. Embryos homozygous for the sll^{7E18} and $sll^{l(3)24533}$ mutations and trans-heterozygotes of these alleles are embryonic lethal. $sll^{l(3)142214}$ was identified in a screen for P-element mutations which, when made homozygous in the ovarian follicle cell layer (Duffy *et al*., 1998), would give rise to dorsalized embryonic progeny. Subsequently, complementation analysis demonstrated that $sll^{l(3)142214}$ is an allele of *sll*. Homozygotes of $sll^{l(3)142214}$ and trans-heterozygotes of this allele with sll^{7E18} or $sll^{l(3)24533}$ are viable and show adult visible phenotypes in the wings.

Mosaics

Germ-line clones were induced in *w*, P{hsFLP}22/+; P{ry⁺t7.2=neoFRT82b, sll}/P{neo FRT82b, ovo^D}* females. Heat shocks were performed during the third larval instar for 2 h at 37°C on two consecutive days. Homozygous mutant clones in imaginal discs were generated by crossing *y^1, w*; P{w⁺mW.hs=en2.4-GAL4}e22c, P{w⁺mC=UAS-FLP1.D}JD1/CyO; P{ry⁺t7.2=neoFRT82b, sll}/TM3, Sb* flies to *P{ry⁺t7.2=neoFRT}82B P{w⁺mC=Ubi-GFP}83*. Larvae were dissected at the third larval instar. Follicle cell clones were generated using the 'directed mosaic' system (Duffy *et al*., 1998). Virgins of the genotype *w; e22c-GAL4, UAS-FLP/+; FRT^{82B} /FRT^{82B} sll^{7E18}* were collected and crossed to Oregon R wild-type males. The e22c-Gal4 enhancer trap line is known to be expressed in the presumptive follicular stem cells.

Misexpression, immunohistochemistry and northern analysis

UAS-wg, UAS-*hh*, *prd-Gal4* and *act-Gal4* lines have been described previously (Selva *et al*., 2001). Primary antibodies used were mouse α-Wg (4D4; Dev. Studies Hybridoma Bank), mouse α-En (4D9; Dev. Studies Hybridoma Bank), rat α-Ci (Motzny and Holmgren, 1995), α-*Drosophila* Golgi (Calbiochem; 1:400), mouse α-Myc (Invitrogen) and rabbit α-Twi (Roth *et al*., 1989). Polyclonal rabbit α-Sll antibodies were raised against the peptide acyl-DQLDAGTSTADKDRC and used at a dilution of 1:2000. Secondary antibodies used in clonal analyses of imaginal discs were α-mouse Cy3 (Amersham) and α-rat Cy5 IgG, H+L (Jackson ImmunoResearch).

Construction of expression plasmids

To add myc-His tags, the *sll* cDNA was amplified by PCR using *sll* N-*Bam*HI (5′-CGAAAGGATCCACATGTACGCCT) and *sll* C-*Apa*I (5′-CCGGGCCCGACAGCCATTTTC) as primers. The resulting cDNA fragment, which has a proline codon instead of the stop codon, was inserted into the mammalian expression vector pcDNA3.1/myc-His (Invitrogen) at its *Bam*HI–*Apa*I sites. For *sll* expression in yeast, a modified pYEX-BX vector (Clontech Laboratories, Palo Alto, CA) was used (Segawa *et al*., 2002). pYEX-*sll/myc*-His was constructed by inserting a 1.4 kb fragment, excised *Bam*HI and *Pme*I from pcDNA3.1-sll/Myc-His, into the *Bam*HI and *Sma*I site of pYEX. *Saccharomyces cerevisiae* YPH500 cells were transformed with pYEX and pYEX-sll/myc-His.

Standard nucleotide–sugar transport and PAPS assay

sll (epitope tagged at the C-terminus with Myc and His6 sequences) was subcloned into the copper-inducible expression vector pYEX-BX and transformed into *S.cerevisiae* strain YPH500 as described (Segawa *et al*., 2002). Expression of *sll* was confirmed by western blotting with anti-Myc antibodies (data not shown). Subcellular fractionation and intact microsomal vesicles were prepared as described previously (Sun-Wada *et al*., 1998) with minor modification (Goto *et al*., 2001). The membrane fractions obtained by centrifugation at 10 000 and 100 000 *g* were combined and used in the transport assay. Yeast microsomal preparations exhibited linearity with protein, time and temperature. In the standard transport assay, microsomes (50 μg of protein) were incubated in 0.1 ml of TSE buffer (10 mM Tris–HCl pH 7.0, 0.8 M glucitol, 2 mM EDTA, 50 mM dimercaptopropanol) containing 1 μM radioactive substrate (6400 Ci/mol unless otherwise specified) at 30°C for 1 min. The PAPS transport, UDP-GlcA transport and GDP-Man transport were carried out using [^{35}S]PAPS (2990 Ci/mol), [1-^{14}C(U)]UDP-GlcA (300 Ci/mol) and GDP-[^{14}C]Man (150 Ci/mol). The reaction was terminated by 10-fold dilution with ice-cold TSE. The radioactive material incorporated into microsomes was trapped on a nitrocellulose filter (Millipore, Bedford, MA) and the radioactivity retained on the filter was measured.

Acknowledgements

We express our thanks to Antonio Giraldez and Stephen Cohen for supplying materials and for their help with the cell culture assays. We thank Sverker Nystedt for the α-Ci antibody and Wilma Martinez Arias for help with northern blotting. D.S. would like to thank Poornima Parameswaran and Jason Goltz for technical assistance. This work is supported by the Swedish Foundation for Strategic Research (SSF) Developmental Biology Programme, providing a junior research group to U.H., the Swedish Research Council VR (U.H.), the Swedish Cancer Foundation (U.H.) and NIH grant AI20941 (S.J.T.). Work in the laboratory of D.S. was supported by NIH grant GM52761.

References

Amiri,A. and Stein,D. (2002) Dorsoventral patterning: a direct route from ovary to embryo. *Curr. Biol.*, **12**, R532–R354.

Baeg,G.H., Lin,X., Khare,N., Baumgartner,S. and Perrimon,N. (2001) Heparan sulfate proteoglycans are critical for the organization of the extracellular distribution of Wingless. *Development*, **128**, 87–94.

Bellaiche,Y., The,I. and Perrimon,N. (1998) Tout-velu is a *Drosophila* homologue of the putative tumour suppressor EXT-1 and is needed for Hh diffusion. *Nature*, **394**, 85–88.

Binari,R.C., Staveley,B.E., Johnson,W.A., Godavarti,R., Sasisekharan,R. and Manoukian,A.S. (1997) Genetic evidence that heparin-like glycosaminoglycans are involved in wingless signaling. *Development*, **124**, 2623–2632.

Capasso,J.M. and Hirschberg,C.B. (1984) Mechanisms of glycosylation and sulfation in the Golgi apparatus: evidence for nucleotide sugar/nucleoside monophosphate and nucleotide sulfate/nucleoside monophosphate antiports in the Golgi apparatus membrane. *Proc. Natl Acad. Sci. USA*, **81**, 7051–7055.

Duffy,J.B., Harrison,D.A. and Perrimon,N. (1998) Identifying loci required for follicular patterning using directed mosaics. *Development*, **125**, 2263–2271.

Fujise,M., Izumi,S., Selleck,S.B. and Nakato,H. (2001) Regulation of dally, an integral membrane proteoglycan and its function during adult sensory organ formation of *Drosophila*. *Dev. Biol.*, **235**, 433–448.

Gerardy-Schahn,R., Oelmann,S. and Bakker,H. (2001) Nucleotide sugar transporters: biological and functional aspects. *Biochimie*, **83**, 775–782.

Goto,S., Taniguchi,M., Muraoka,M., Toyoda,H., Sado,Y., Kawakita,M. and Hayashi,S. (2001) UDP-sugar transporter implicated in glycosylation and processing of Notch. *Nat. Cell Biol.*, **3**, 816–822.

Häcker,U., Lin,X. and Perrimon,N. (1997) The *Drosophila* sugarless gene modulates Wingless signaling and encodes an enzyme involved in polysaccharide biosynthesis. *Development*, **124**, 3565–3573.

Haerry,T.E., Heslip,T.R., Marsh,J.L. and O'Connor,M.B. (1997) Defects in glucuronate biosynthesis disrupt Wingless signaling in *Drosophila*. *Development*, **124**, 3055–3064.

Hannon,G.J. (2002) RNA interference. *Nature*, **418**, 244–251.

Hirschberg,C.B. and Snider,M.D. (1987) Topography of glycosylation in

the rough endoplasmic reticulum and Golgi apparatus. *Annu. Rev. Biochem.*, **56**, 63–87.

Huang,M.A., Rehm,E.J. and Rubin,G.M. (2000) Recovery of DNA sequences flanking P-element insertions: inverse PCR and plasmid rescue. In Sullivan.,W., Ashburner,M. and Hawley,R.S. (eds), *Drosophila Protocols*. Cold Spring Harbor Laboratory Press, Cold Spring Harbor, NY, pp. 429–437.

Irvine,K.D. (1999) Fringe, Notch and making developmental boundaries. *Curr. Opin. Genet. Dev.*, **9**, 434–441.

Ishida,N., Miura,N., Yoshioka,S. and Kawakita,M. (1996) Molecular cloning and characterization of a novel isoform of the human UDP-galactose transporter and of related complementary DNAs belonging to the nucleotide–sugar transporter gene family. *J. Biochem. (Tokyo)*, **120**, 1074–1078.

Jullien,D., Crozatier,M. and Kas,E. (1997) cDNA sequence and expression pattern of the *Drosophila melanogaster* PAPS synthetase gene: a new salivary gland marker. *Mech. Dev.*, **68**, 179–186.

Khare,N. and Baumgartner,S. (2000) Dally-like protein, a new *Drosophila* glypican with expression overlapping with wingless. *Mech. Dev.*, **99**, 199–202.

Lin,X. and Perrimon,N. (1999) Dally cooperates with *Drosophila* Frizzled 2 to transduce Wingless signalling. *Nature*, **400**, 281–284.

Lin,X., Buff,E.M., Perrimon,N. and Michelson,A.M. (1999) Heparan sulfate proteoglycans are essential for FGF receptor signaling during *Drosophila* embryonic development. *Development*, **126**, 3715–3723.

Lyle,S., Stanczak,J., Ng,K. and Schwartz,N.B. (1994) Rat chondrosarcoma ATP sulfurylase and adenosine 5′-phosphosulfate kinase reside on a single bifunctional protein. *Biochemistry*, **33**, 5920–5925.

Mandon,E.C., Milla,M.E., Kempner,E. and Hirschberg,C.B. (1994) Purification of the Golgi adenosine 3′-phosphate 5′-phosphosulfate transporter, a homodimer within the membrane. *Proc. Natl Acad. Sci. USA*, **91**, 10707–10711.

Miura,N., Ishida,N., Hoshino,M., Yamauchi,M., Hara,T., Ayusawa,D. and Kawakita,M. (1996) Human UDP-galactose translocator: molecular cloning of a complementary DNA that complements the genetic defect of a mutant cell line deficient in UDP-galactose translocator. *J. Biochem. (Tokyo)*, **120**, 236–241.

Monigatti,F., Gasteiger,E., Bairoch,A. and Jung,E. (2002) The Sulfinator: predicting tyrosine sulfation sites in protein sequences. *Bioinformatics*, **18**, 769–770.

Motzny,C.K. and Holmgren,R. (1995) The *Drosophila* cubitus interruptus protein and its role in the wingless and hedgehog signal transduction pathways. *Mech. Dev.*, **52**, 137–150.

Mullor,J.L., Calleja,M., Capdevila,J. and Guerrero,I. (1997) Hedgehog activity, independent of decapentaplegic, participates in wing disc patterning. *Development*, **124**, 1227–1237.

Nakato,H., Futch,T.A. and Selleck,S.B. (1995) The division abnormally delayed (dally) gene: a putative integral membrane proteoglycan required for cell division patterning during postembryonic development of the nervous system in *Drosophila*. *Development*, **121**, 3687–3702.

Nilson,L.A. and Schüpbach,T. (1998) Localized requirements for windbeutel and pipe reveal a dorsoventral prepattern within the follicular epithelium of the *Drosophila* ovary. *Cell*, **93**, 253–262.

Ozeran,J.D., Westley,J. and Schwartz,N.B. (1996) Identification and partial purification of PAPS translocase. *Biochemistry*, **35**, 3695–3703.

Park,Y., Rangel,C., Reynolds,M.M., Caldwell,M.C., Johns,M., Nayak,M., Welsh,C.J., McDermott,S. and Datt,S. (2003) *Drosophila* perlecan modulates FGF and hedgehog signals to activate neural stem cell division. *Dev. Biol.*, **253**, 247–257.

Peifer,M., Rauskolb,C., Williams,M., Riggleman,B. and Wieschaus,E. (1991) The segment polarity gene armadillo interacts with the wingless signaling pathway in both embryonic and adult pattern formation. *Development*, **111**, 1029–1043.

Perrimon,N. (1994) The genetic basis of patterned baldness in *Drosophila*. *Cell*, **76**, 781–784.

Perrimon,N. and Bernfield,M. (2000) Specificities of heparan sulfate proteoglycans in developmental processes. *Nature*, **404**, 725–729.

Rorth,P. (1998) Gal4 in the *Drosophila* female germline. *Mech. Dev.*, **78**, 113–118.

Roth,S., Stein,D. and Nusslein-Volhard,C. (1989) A gradient of nuclear localization of the dorsal protein determines dorsoventral pattern in the *Drosophila* embryo. *Cell*, **59**, 1189–1202.

Segawa,H., Kawakita,M. and Ishida,N. (2002) Human and *Drosophila* UDP-galactose transporters transport UDP-N-acetylgalactosamine in addition to UDP-galactose. *Eur. J. Biochem.*, **269**, 128–138.

Selva,E.M., Hong,K., Baeg,G.-H., Beverley,S.M., Turco,S.J., Perrimon,N. and Häcker,U. (2001) Dual role of the fringe connection gene in both heparan sulfate and fringe-dependent signalling events. *Nat. Cell Biol.*, **3**, 809–815.

Sen,J., Goltz,J.S., Stevens,L. and Stein,D. (1998) Spatially restricted expression of pipe in the *Drosophila* egg chamber defines embryonic dorsal–ventral polarity. *Cell*, **95**, 471–481.

Spring,J., Paine-Saunders,S.E., Hynes,R.O. and Bernfield,M. (1994) *Drosophila* syndecan: conservation of a cell-surface heparan sulfate proteoglycan. *Proc. Natl Acad. Sci. USA*, **91**, 3334–3338.

Stanley,H., Botas,J. and Malhotra,V. (1997) The mechanism of Golgi segregation during mitosis is cell type-specific. *Proc. Natl Acad. Sci. USA*, **94**, 14467–14470.

Strigini,M. and Cohen,S.M. (1997) A Hedgehog activity gradient contributes to AP axial patterning of the *Drosophila* wing. *Development*, **124**, 4697–4705.

Sun-Wada,G.H., Yoshioka,S., Ishida,N. and Kawakita,M. (1998) Functional expression of the human UDP-galactose transporters in the yeast *Saccharomyces cerevisiae*. *J. Biochem. (Tokyo)*, **123**, 912–917.

Toyoda,H., Kinoshita-Toyoda,A., Fox,B. and Selleck,S.B. (2000) Structural analysis of glycosaminoglycans in animals bearing mutations in sugarless, sulfateless and tout-velu. *Drosophila* homologues of vertebrate genes encoding glycosaminoglycan biosynthetic enzymes. *J. Biol. Chem.*, **275**, 21856–21861.

Tsuda,M. *et al*. (1999) The cell-surface proteoglycan Dally regulates Wingless signalling in *Drosophila*. *Nature*, **400**, 276–280.

Received April 4, 2003; revised May 14, 2003; accepted May 20, 2003